IEEE Access
Multidisciplinary | Rapid Review | Open Access Journal

Received 30 June 2023, accepted 25 August 2023, date of publication 11 September 2023, date of current version 15 September 2023.

Digital Object Identifier 10.1109/ACCESS.2023.3313939

RESEARCH ARTICLE

Microwave Biomedical Sensors With Stable Response: Basic Idea and Preliminary Numerical Assessments for Blood Glucose Monitoring

SANDRA COSTANZO[1,2,3,5], (Senior Member, IEEE), ANTONIO CUCCARO[1,3], ANGELA DELL'AVERSANO[4], GIOVANNI BUONANNO[1,3], (Member, IEEE), AND RAFFAELE SOLIMENE[4,5,6], (Senior Member, IEEE)

[1]Department of Informatics, Modeling, Electronics and Systems Engineering (DIMES), University of Calabria, 87036 Rende, Italy
[2]Institute for Electromagnetic Sensing of the Environment (IREA), National Research Council of Italy (CNR), 80124 Naples, Italy
[3]Inter-University National Research Center on Interactions between Electromagnetic Fields and Biosystems (ICEmB), 16145 Genoa, Italy
[4]Department of Engineering, University of Campania "Luigi Vanvitelli," 81100 Aversa, Italy
[5]Consorzio Nazionale Interuniversitario per le Telecomunicazioni, 43124 Parma, Italy
[6]Department of Electrical Engineering, Indian Institute of Technology Madras, Chennai 600036, India

Corresponding author: Sandra Costanzo (costanzo@dimes.unical.it)

This work was supported in part by Ministero dell'Università e della Ricerca (MUR), Italy, through the Project PNRR PE8—Conseguenze e sfide dell'invecchiamento "Ageing well in an Ageing Society (Age-IT);" and in part by Programma Operativo Nazionale (PON) Ricerca e Innovazione (2014–2020) through the Project Non-invasive Electromagnetic Green Devices and Methods for Advanced Medical Diagnostics.

ABSTRACT Microwave sensors are gaining increasing interest in blood glucose detection, for their potential ability to perform a continuous non-invasive monitoring of the glucose concentration, by relating the change in the blood dielectric properties to a variation in the glucose level. Usually, the involved body part (phantom) is placed on the sensor to perform the reading. However, the placement modality, as well as other external factors not related to the blood glucose concentrations (BGC) (i.e. system noise, environmental temperature, human tissues variations other than blood tissue) may also have an effect on the sensor response, due to the change in the propagation path of the electromagnetic field inside the body part under test. In this work, the variation effects induced on the microwave sensor response by the changes in the thickness and the dielectric properties of skin and fat tissues are analyzed and faced. In particular, to mitigate the above drawback in terms of sensor instability, a solid "matching layer" is interposed between the resonant sensor and the phantom under test. A specific optimization procedure is performed to design microwave sensors with a stable response not influenced by variations in tissues different from the blood. Various sensors configurations with related resolution metrics are considered to assess the proposed idea and design methodology. Numerical results confirm the possibility to achieve a good trade-off between the measurement stability against undesired phantom variations and the sensitivity toward blood glucose levels, allowing to discriminate concentrations in the range of [100-300] mg/dL.

INDEX TERMS Antennas, electromagnetics, propagation, measurements.

I. INTRODUCTION

Diabetes is a chronic condition to be diagnosed and properly treated for preventing complications [1], [2], such as blindness, cardiovascular diseases and a potential increased risk of stroke and lower limb amputation.

The most widely used method for measuring blood glucose level consists in pricking a finger and putting a drop of blood onto a strip test. This method is invasive, uncomfortable and the number of measurements per day is limited.

The associate editor coordinating the review of this manuscript and approving it for publication was Mohamed Kheir.

To overcome this limitations, a great deal of research has been developed. For example, in [3] and [4], tears and urine analysis has been considered. Though, these approaches allow for non-invasive glucose level monitoring, the glucose level in saliva, sweat and eye tears is much lower than in the blood [5]. What is more, those methods are not suited to achieve continuous monitoring.

Non-invasive continuous monitoring is instead desirable since diabetics must measure blood glucose concentration regularly, several times per day, i.e., before and two hours after each meal, prior to sleeping, etc. [3]. To this end, microwave sensors are gaining increased interest since they can potentially provide a valid tool to achieve continuous non-invasive glucose monitoring, without upsetting the patient daily activity. For example, the possibility of non-invasively determining the glucose concentration through the variation of blood dielectric parameters (conductivity is detected through changes in the corresponding eddy current [6]) has been investigated in [6].

Microwave sensors exploit the interaction of electromagnetic waves with biological tissues [6], [7]. Since blood permittivity weakly changes with glucose concentration [8], [9], [10], [11], [12], [13] research usually focuses on the design of high-Q factor sensors whose sharp response allows to more easily track the resonance frequency shift due to glucose concentration changes [14], [15], [16], [17]. In [18] a sensor with high Q-factor is validated against solid material samples for single and multi-layer configurations, instead in [19] and [20] material properties are determined by a phase variation sensor implemented in microstrip technology. A dual frequency microwave split ring resonator is show in [21] for liquid samples, whereas a similar strategy is proposed in [22], where a two resonant frequency dual-sensing sensor is presented for non-invasive glucose concentration determination. Microwave resonators of various shapes are reported in [23], [24], [25], [26], and [27]. Further results can be found in [28] and [29]. Other interesting configurations, based on split ring resonator, and exhibiting high Q-factors, can be found in [30] and [31]. Also, we mention that suitable signal processing can be employed to sharp the sensor's response, thus remedying to possible low Q-factors [32], [33], [34], [35].

A crucial question of this type of sensors is that their response can depend by factors besides the properties that actually should be tracked. Environment conditions (i.e., temperature, humidity, etc.), sensor's pose (with respect to the material sample to be investigated), deviation of the properties of the sample under test from the assumed nominal ones, etc. are typical issues that, if not properly addressed, can lead to wrong estimations.

Environment effects can be mitigated by employing a reference sensor that is then used to calibrate the one in charge of material characterization [36], whereas the influence of fingerprints and fingertip localization on the sensor area have been analyzed in detail in [37] and [38]. Even more critical is the case in which the properties of the sample under test (besides the one that should be tracked) deviate from the nominal ones adopted during the sensor design stage. This is particularly important for sensors intended to work in contact with the human body. In this case, the dielectric permittivity and thickness of various tissue layers (i.e., skin, fat, etc.) hardly coincide with the theoretical ones. As a result, the entailed resonance frequency shift can be as large as, even not greater than, the one due to the variation of the glucose level.

This crucial aspect seems to have been underrated in the pertinent literature. Here we just focus on this issue. In particular, we are interested in studying whether and at what extent variations/uncertainties occurring into the non-targeted tissues affect the sensor's response. In particular, here we deepen a study presented in [39].

To this end, we perform a numerical analysis by considering three different sensors borrowed from literature: a standard patch antenna [40], a patch resonator [41] and a microwave split ring resonator [42]. This is done in order to appreciate the impact of the sensor's type. The sensors' responses are computed when they are put against a commonly employed four-layered numerical phantom [41] consisting of skin, fat, blood and muscle layers. In particular, the size and the properties of the tissues are set to accommodate the working frequency and the sensing area of the different considered sensors. In order to check sensors' stability, the properties of the tissues are perturbed with respect to the ones assumed for sensors' design their responses computed as the blood glucose concentration changes. It is shown that tissue perturbation actually may introduce frequency shifts which can be even larger than the ones due to glucose concentration changes. This circumstance can clearly impair practical application of such sensors. Therefore, a strategy for mitigating such a drawback is proposed. To this end, here we explore the possibility of obtaining stable (against tissues' perturbation) sensors' responses by introducing a superstrate layer, that is a matching layer between the sensors and the phantom. Numerical results show that the loaded sensors exhibit relatively stable responses (as compared to their unloaded counterparts) at the cost of a reduced resolution. Therefore, the simple proposed solution can potentially mitigate the estimation errors due to uncertain tissue properties.

The rest of the paper is organized as follows. Section II is devoted to detail the problem we are concerned with, the description of the synthetic phantom and the used performance metrics. In Section III the three different sensors under consideration are briefly described along with their superstrate loaded counterparts. Section IV reports the numerical analysis. Conclusions and Future Developments end the paper.

II. PROBLEM DESCRIPTION

The design of microwave biosensors requires the knowledge of the electromagnetic properties of the biological tissues

involved in the propagation mechanism. However, in practical cases, the actual dielectric properties and thicknesses of the biological tissues are at best known with some degree of uncertainty and can change from person to person. For example, across the population there can be a significant variation in the skin properties (even depending on the body locations where the sensor should be placed), related to gender, age, ethnicity, physical health and fitness status. Such changes make it is difficult to establish a clear link between the sensor's response and the property that has to be estimated/tracked. Temperature and humidity can impact the sensor's as well. Environment condition effect can be mitigated by employing two sensors: the first one is used to get the response due to the environment effect and it is then used to calibrate the second one in contact to the patient and in charge of glucose concentration estimation [36].

However, a microwave sensor should be able to accommodate or to be resilient (at some extent) to tissues' variations as well. Indeed, at least the skin thickness variations [46] should be considered, although it is better to account for changes in all tissues that are interested by the electromagnetic fields. In fact, a crucial question in microwave sensor for blood glucose concentration is to establish the link between the frequency shift (or other measured parameter) to the targeted blood glucose concentration. To this end, a standard way is to calibrate the sensor's response by measuring the frequency shift and attaching it to the glucose concentration returned by a reference measurement, typically, obtained via a glucometer, as done for example in [21]. Now, since the shift in the resonance frequency due to change in tissues properties can be of the same order as the one due to chances in the glucose concentration, it is clear that it is very hard to relate to the frequency shift to the targeted blood glucose concentration only.

Here, we are concerned in assessing the role of uncertainties on tissues' properties for microwave blood glucose concentration sensors. To this end, we conduct a numerical analysis by considering three different microwave sensors (described in more detail in the sequel): a patch antennas working at the nominal frequency of 2.3 GHz, a patch resonator working at the nominal frequency of 2.4 GHz and a split ring resonator designed to work at 6 GHz. Note that the first two frequencies belong to the standard ISM band, while the additional band around 6 GHz is considered to meet further wireless and/or biometric operations possibly required when considering the microwave sensor embedded into a complete wireless biomedical device. The responses of the three mentioned sensors are analyzed when in contact with a four-layered phantom when the tissues' properties change with respect to the nominal ones. Classical metrics are employed to quantify the sensors' performance, such as the Q factor and the resolution/sensitivity. Also, since here we are mainly focused in studying how the sensors' responses vary with the tissues' properties a stability metrics is also considered.

A. THE PHANTOM

In order to easily perform the numerical analysis, it is convenient to be built the phantom by trading-off complexity and physical target description. To this end, we consider a phantom commonly employed in literature [13] that consists of four layers accounting for skin, fat, blood and muscle layers. The interfaces among different tissue layers are assumed planar; this is reasonable since the considered sensors are relatively small in size.

The transversal size of the phantom as well as the dielectric and conductivity of the layers are adjusted according to the sensing area and the working frequencies of the different considered sensors. In particular, to set the properties of the skin, fat and muscle layers we employ the 4 poles Cole-Cole dielectric model reported in [12]. For the blood layer, instead, we employ the model presented in [29].

As mentioned above, we are interested in analyzing the sensors' responses as the phantom properties change with respect to the nominal ones. For the sake of simplicity (and as it is usually done in literature where the muscle tissue is even neglected [47]) the muscle tissue properties are kept constant. Therefore, in the following analysis, only the properties of the skin, the fat and of the blood layers will be changing. The intended analysis of course still requires a multi-parametric study. To simplify the matter, and at the same time to give a concise presentation of the results, we limit to show selected but representative cases. In particular, three different values are considered for the equivalent dielectric permittvity of the skin and fat layers. Also three different thicknesses are considered for such layers.

The dielectric and conductivity properties of the tissues at the three working frequencies as well as their thicknesses are summarized in TABs. 1 and 2. The average values of the relative dielectric permittivity, conductivity and thickness, that is ϵ_{rav}, σ_{av} and δ_{av}, are assumed as the nominal parameters that are employed for sensors' design. Also, the properties of the skin, at a given frequency, i.e., $\epsilon_{skin_{min}}$, $\sigma_{skin_{min}}$, $\epsilon_{skin_{max}}$, $\sigma_{skin_{max}}$ and $\epsilon_{skin_{av}}$, $\sigma_{skin_{av}}$, correspond to the case of dry skin, wet skin and the average among them, respectively. As to the properties of the fat layer, the variations could have been set according to the values returned by different models reported in literature [11]. However, in order to always employ the same model, here we have preferred to perturb the values given by the model in [12] by an amount ranging from 2% to 3% (depending on the working frequency). Finally, we remark that the blood parameters reported in TAB. 1 corresponds to the zero glucose level [29].

Since the sensors are intended for blood glucose concentration (BGC) monitoring, when glucose level deviates from the one of the reference phantom, the relative permittivity and conductivity of blood layer will be varying according to the double pole Cole-Cole modified dielectric model given in [13]. The corresponding blood electromagnetic parameters are reported in TAB. 3, for three different glucose concentrations. These concentrations have been selected since they

TABLE 1. Dielectric and conductivity properties of the phantom tissues at $f_1 = 2.3$ GHz, $f_2 = 2.4$ GHz and $f_3 = 6$ GHz. Muscle and fat tissues are kept fixed at ϵ_{rav} and σ_{av} values.

	ϵ_{rmax}			ϵ_{rav}			ϵ_{rmin}			σ_{max} [S/m]			σ_{av} [S/m]			σ_{min} [S/m]		
Tissue	f_1	f_2	f_3	f_1	f_2	f_3	f_1	f_2	f_3	f_1	f_2	f_3	f_1	f_2	f_3	f_1	f_2	f_3
Skin	43.04	42.85	38.38	41.00	40.12	36.67	38.13	38.00	34.95	1.50	1.59	4.54	1.45	1.53	4.21	1.40	1.46	3.88
Fat	5.45	5.43	5.09	5.30	5.28	4.94	5.15	5.13	4.79	0.12	0.118	0.323	0.098	0.105	0.306	0.085	0.092	0.297
Muscle				52.93	52.73	48.22							1.63	1.738	5.2			
Blood				61.43	58.34	61.43							3.18	2.48	3.18			

TABLE 2. Thickness of the phantom tissues. muscle and fat size are kept fixed at δ_{av} value.

Tissue	$\delta_{max}[mm]$	$\delta_{av}[mm]$	$\delta_{min}[mm]$
Skin	0.8	1.5	2
Fat	0.5	1.0	1.5
Muscle		15.0	
Blood		2.5	

mimic the transition from healthy to pathological situations, and they are in agreement with the study reported in [9]. In particular, glucose levels up to 216 mg/dl can be considered healthy.

B. METRICS

In order to compare the different sensors, metrics commonly employed in literature are considered in the sequel. In particular, the sensor's resolution/sensitivity can be estimated as

$$SR = \frac{|f_0(C_{min}) - f_0(C_{max})|}{C_{max} - C_{min}} = \frac{\Delta f}{\Delta C} \tag{1}$$

where C_{max}, C_{min} and ΔC are the minimum, the maximum and the interval within which the blood glucose concentration varies, whereas $f_0(C_{min})$ and $f_0(C_{max})$ and Δf the resonance frequencies detected by the sensor and the corresponding frequency interval.

SR is usually paired with the Q-factor. This parameter can be defined by taking into account the phase information on the scattering parameters, as shown in [48], or using traditional definition as in [18], namely:

$$Q = \frac{f_0}{\Delta_{3dB}} \tag{2}$$

where the detected resonance frequency is normalized by the 3 dB bandwidth around it. A high Q-factor is desirable since this entails a sharper resonance frequency estimation.

The response of a microwave sensor, and hence the metrics defined above, depends not only on the blood glucose concentration but also on the properties of the other tissues. If the latter deviate from the nominal ones the achievable performance changes. Therefore, to seriously assess the achievable performance it is mandatory to study the metrics above not only as the blood glucose concentration changes but even when other tissue properties have some degree of uncertainty.

The robustness of sensor's response can be assessed by looking at how *SR* and Q change with tissue uncertainties. The sensor can be considered robust if *SR* and Q weakly changing as tissues' properties slightly change. However, it may happen that even when *SR* and Q are relatively stable, the resonance frequency corresponding to a given blood glucose concentration changes when tissues are slightly perturbed. As a consequence, it would be difficult to discern if the frequency shift is due to glucose concentration variation or to a mismatch between the nominal tissue values and the actual ones. Therefore, a better and more precise way to assess the robustness is by the following metrics

$$RM = \frac{\max_i f_0(C) - \min_i f_0(C)}{f_{0N}} \times 100 \tag{3}$$

where index i spans over N different tissue configurations with permittivity/conductivity and/or layer thickness perturbed with respect to the nominal values, $f_0^i(C)$ are the corresponding resonance frequencies (at the fixed blood glucose concentration C) and f_{0N} is the sensor's resonance frequency corresponding to the tissue nominal values. Ideally, one would like that *RM* be zero.

III. SUPERSTRATE-LOADED MICROWAVE SENSORS

Tissue perturbation affect microwave sensors' responses. To assess if and at what extent this can impair to track blood glucose concentration a multi-parametric analysis should be carried out. Also, different sensors can be affected differently by tissue perturbation. In the previous section, we have already described the phantom and the tissue perturbations that are going to be considered. As to the sensors, three different sensors will be considered: a patch antenna (PA), a patch resonator (PR) and split ring resonator (SRR). In particular, for each sensor two different versions are designed, i.e., without and with a loading superstrate layer. In particular, the superstrate is used to mitigate resonance frequency shift due to tissues' perturbation.

All sensors are designed in miscrostrip technology. As to the superstrate, we have two degrees of freedom, i.e., the material and the thickness. In order to simplify the study, the relative dielectric permittivity is set equal to 10, so to realize the best matching condition with the biological tissue. Moreover, materials exhibiting such a permittivity are easily available, and they can be found, for example, as a filament for a 3D printer [49]. The superstrate thickness is determined by imposing that the resonance frequency remains unchanged when passing to the loaded sensor configuration, as compared to the reference phantom with nominal tissues features and zero blood glucose concentration. The sensors design, as well

TABLE 3. Dielectric and conductivity of the blood tissues for different glucose concentration.

	2.3 GHz		2.4 GHz		6 GHz	
BGC [mg/dl]	$\epsilon_{r_{blood}}$	σ_{blood} [S/m]	$\epsilon_{r_{blood}}$	σ_{blood} [S/m]	$\epsilon_{r_{blood}}$	σ_{blood} [S/m]
100	58.6800	1.2828	58.4600	1.4010	57.6600	1.9000
200	50.2300	1.3047	50.0200	1.4250	49.3400	1.9300
300	41.7400	1.3267	41.5900	1.4490	41.0200	1.9600

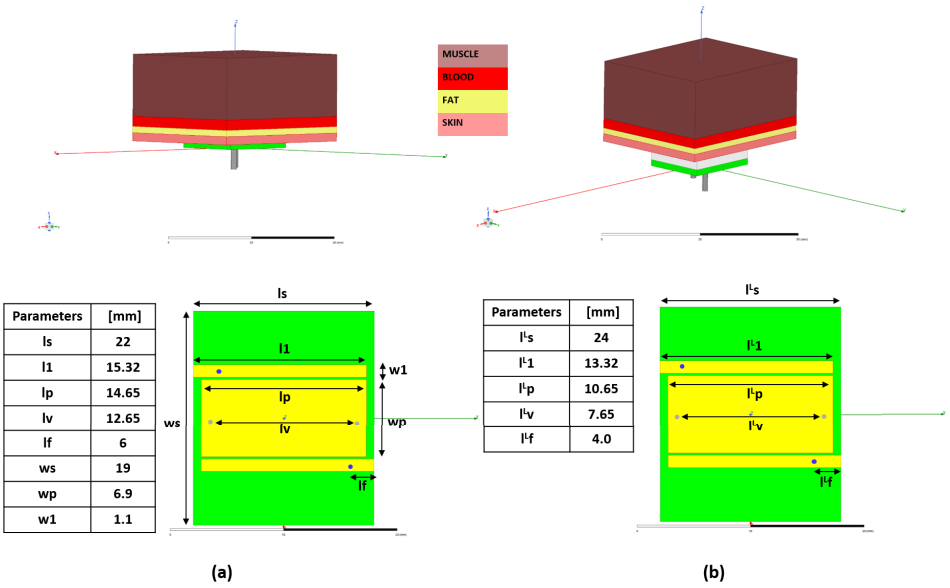

FIGURE 1. Sensors and phantom: (a) patch resonator (PR) and (b) loaded patch resonator (LPR). Both sensors work in direct contact with complete phantom structure.

as the determination of the superstrate thickness are achieved by numerical simulations on the HFSS software.

For convenience, in the following, the loaded sensors will be denoted as LPA (loaded patch antenna), LPR (loaded patch resonator) and LSRR (loaded split ring resonator), respectively.

A. PR AND LPR

The PR sensors and its loaded version are shown in Fig. 1 (panel (a) and (b)). In particular, both the sensors have been designed to resonate at 2.4 GHz and by considering a Rogers *R*03010 substrate having $\epsilon_{=}10.2$ $\tan\delta = 0.0023$ and thickness $h_s = 1.6$ mm. More in detail, the PR sensor consists of a patch resonator short-circuited through via holes at the two edges and feed by two coupled miscrostrip lines terminated by coaxial cables. The sensor has been designed by considering it working in contact with the phantom and by setting the tissue layer parameters according to the nominal values (see previous section) at 2.4 GHz. The loading superstrate of LPR has been optimized by numerical simulations so to have the same resonance frequency as RP. The resulting sensor is shown in Fig. 1 (panel (b)) along with the loading superstrate whose thickness was found to be 5 mm.

The sizes of the sensors (and the relative sensing areas) can be appreciated in panels (c) and (d) and are approximately of 35×35 mm^2, hence they are suited to be put on the back of a hand, on a shoulder and in general on body places large enough to allow for a correct sensor's placement.

B. PA AND LPA

The second sensor under consideration is a standard patch antenna over a FR4 substrate with $\epsilon_r = 4.4$, $\tan\delta = 0.012$ and thickness $h_s = 1.6$ mm. By following the same approach as above, the patch antenna is designed by considering the nominal phantom parameters. This choice, according to well-known design rules reported in [25], allows to obtain a compact resonance antenna at 2.3 GHz. A coaxial probe feeding is used to facilitate the sensor positioning on the human body. Moreover, the feed can be placed at any desired location on the patch in order to match the cable impedance with the antenna input impedance. The superstrate thickness has been determined by numerical simulations and it was found to be also in this case of 5 mm.

The PA and the LPA sensors are shown in Fig. 2 along with their cross section views to appreciate the physical dimensions.

C. SRR AND LSRR

The last considered sensor is a split ring resonator with a T-shaped structure aimed at increasing the sensor's sensitivity. In this case, the substrate is a Rogers *RO*4003 with $\epsilon_{=}3.38$, $\tan\delta = 0.0027$ and $h_s = 0.508$ mm.

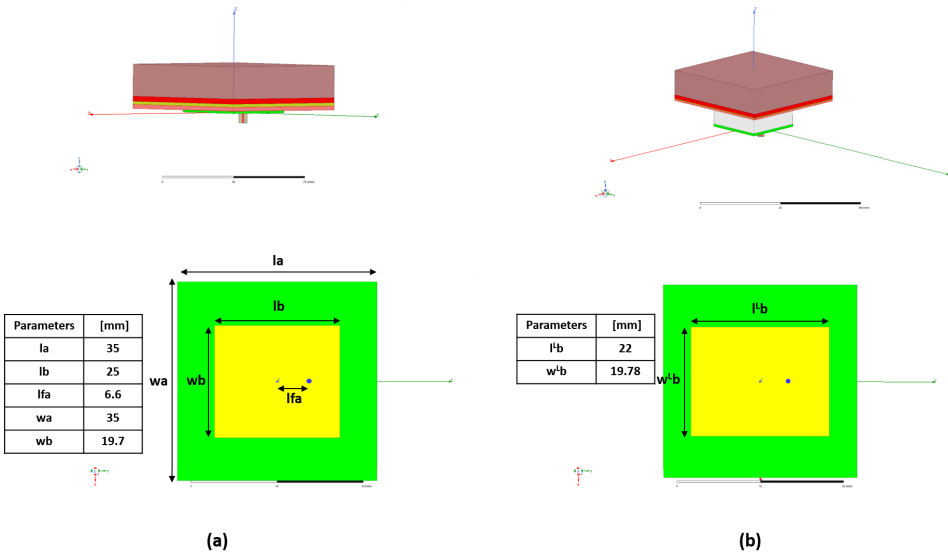

Parameters	[mm]
la	35
lb	25
lfa	6.6
wa	35
wb	19.7

Parameters	[mm]
l'b	22
w'b	19.78

FIGURE 2. Sensors and phantom: (a) patch antenna (PA) and (b) loaded patch antenna (LPA). Both sensors work in direct contact with complete phantom structure.

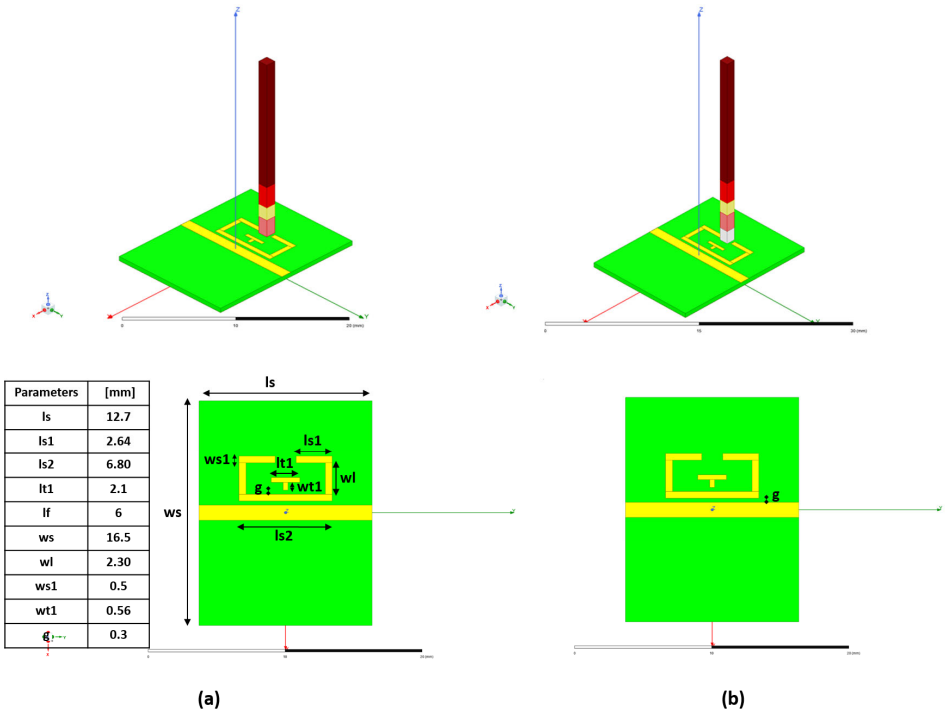

Parameters	[mm]
ls	12.7
ls1	2.64
ls2	6.80
lt1	2.1
lf	6
ws	16.5
wl	2.30
ws1	0.5
wt1	0.56
g	0.3

FIGURE 3. Sensors and phantom: (a) Split ring resonator (SRR) and loaded slit ring resonator (LSRR). Both sensors work in direct contact with complete phantom structure.

It is noted that now the sensing area is the gap of the ring resonator. Accordingly, this type of sensor is better suited for being located over a finger tip. Also, the loading superstrate loading layer as well as phantom need to be put only in correspondence of the gap. In particular, in this case the loading thickness is found to be 1.5 mm. A pictorial view of the SRR and LSRR sensors against the nominal phantom are reported in Fig. 3. Note that, in this case the transverse size of the phantom is adjusted so to match the reduced sensing area.

IV. NUMERICAL ANALYSIS

In this section we turn to check the performance, and in particular the robustness of loaded sensors against skin and

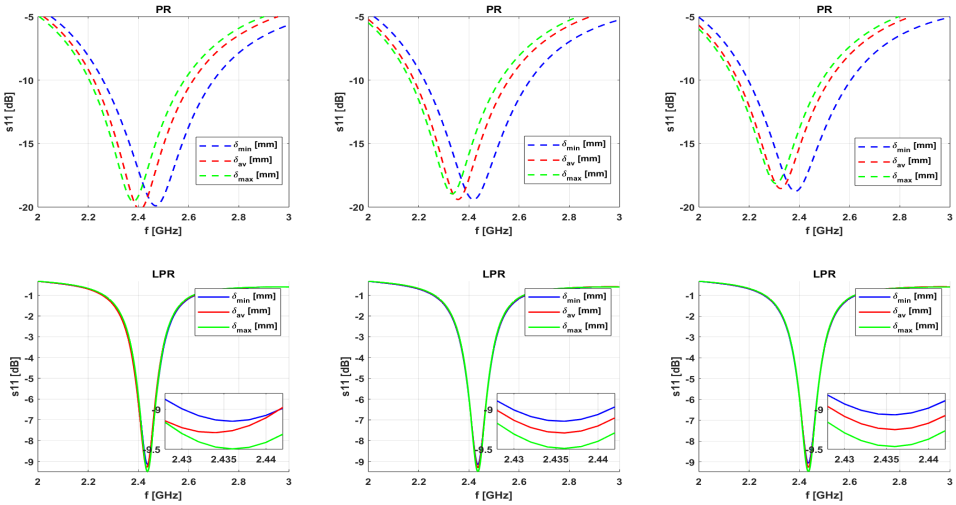

FIGURE 4. Comparison between the PR and LPR responses for $C = 0$ when the skin and fat layers are perturbed from their nominal values. The panels on the left, middle and right columns refer to ϵ_{skin}, σ_{skin}, ϵ_{fat}, σ_{fat} set according to the minimum, average and maximum values reported in TAB. 1, respectively. For each cases, minimum, average and maximum skin and fat layer thickness (reported in TAB. 2) are considered.

fat tissue variations, To this end, we consider phantoms with different parameters as described in the previous section.

The results will be presented by showing the behaviours of the scattering parameters and by computing the metrics described above. More in detail, the S_{11} behaviors will be reported only for the PR and LPR sensors. Similar behaviours have been obtained for the other two types of sensors, and hence, for the sake of shortness, have been omitted here.

A. ILLUSTRATIVE CASE: PR VS LPR

The first example is shown in Fig. 4. It refers to the case of $C = 0$, whereas the properties of the skin and the fat layers are changed. In particular, the panels on the left, middle and right columns refer to the case the dielectric permittivity and conductivity of the skin and fat layers are set to the minimum, average and maximum values as described in TAB. 1. Moreover, for each panels the cases the skin and fat thicknesses are set according to their minimum, average and maximum values (see TAB. 2) are all considered.

In this case, the sensor is robust if the resonance frequency remains stable. Looking at such a figure, it is evident how the resonance frequency of the LPR sensor is weakly dependent on the changes in the phantom properties and practically coincides with the design resonance frequency of 2.4 GHz. By contrary, the resonance frequency of the PR sensor shows significant deviations from the design frequency, especially when the thicknesses change with respect to the nominal ones. Finally, it noted that the LPR responses are much sharper than the ones of PA. Eventually, it can be concluded that the introduced superstrate loading layer actually allows to make the sensor's response stable against small perturbations occurring in the properties of the nominal phantom.

The arising question is whether the gained sensor's stability can reduce the ability to detect shift in the resonance frequency when the blood glucose concentration varies. To this end, as illustrative examples, we consider the cases reported in Figs. 5 and 6. In particular, in order to facilitate the display of the results, in Fig. 5 only the dielectric and conductivity parameters of the skin and the fat layers are changed, whereas the layer thicknesses are keep at the nominal values. In Fig. 6, instead, the dielectric and conductivity parameters are set to the nominal ones whereas the thicknesses are varied. More in detail, in Fig. 5, each panels show the sensors' response as the skin and fat thickness vary (see TAB. 2; the panels on the left, middle and right columns have been obtained by setting the dielectric permittivity and conductivity of the skin and fat layers according to the minimum, average and maximum values reported in TAB. 1, respectively. Instead, in Fig. 6, the skin and fat layer electromagnetic properties are keep at the nominal (average) values wheres their thickness vary from the minimum (panels on the left column) to maximum (panels on the right column) values, according to TAB. 2.

From such figures the following conclusions can be drawn. The PR sensor shows larger differences between the resonance frequencies as the blood glucose concentration changes. This entails better resolution than the LPR. However, the LPR responses are much more sharp and hence more precise resonance frequency estimations are achieved. What is more, for a given blood glucose concentration, the LPR resonance frequencies are very stable as the phantom parameters are different from the nominal ones.

B. METRICS ANALYSIS

Previous examples just provided a qualitative understanding of the usefulness of loading a microwave sensor. Also, as mentioned above, for the sake of brevity, we have limited to address the comparison between the PR and LPR sensors.

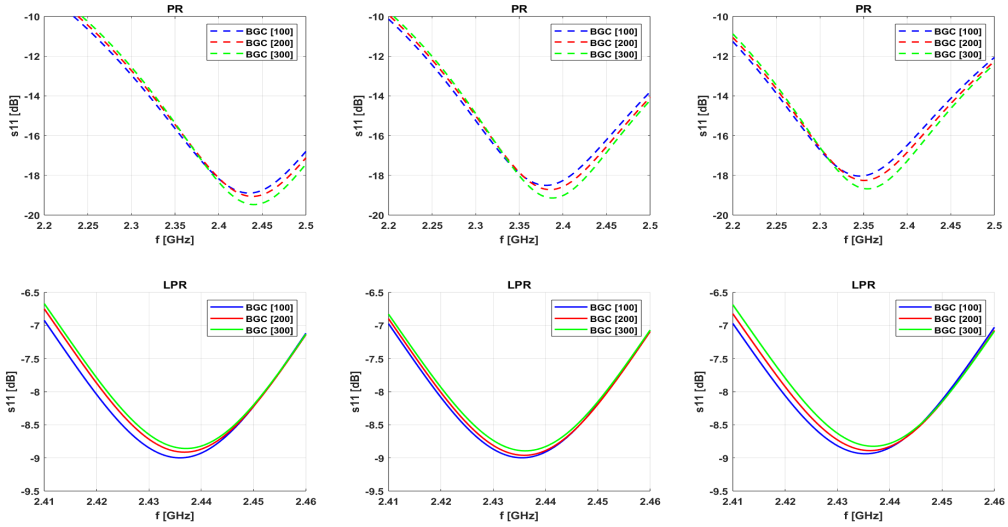

FIGURE 5. Comparison between the PR and LPR responses for three blood glucose concentrations. The panels on the left, middle and right columns refer to ϵ_{skin}, σ_{skin}, ϵ_{fat}, σ_{fat} set according to the minimum, average and maximum values reported in TAB. 1, respectively. For each cases, the skin and fat layer thickness have been set to the nominal values (i.e., the average values reported in TAB. 2). Finally, the properties of the blood for the three different concentrations has been set as reported in TAB. 3.

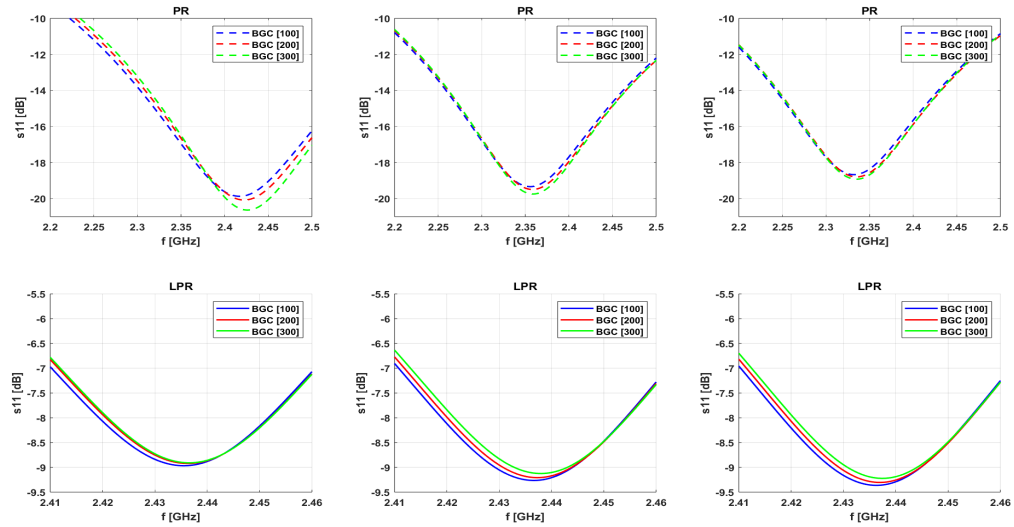

FIGURE 6. Comparison between the PR and LPR responses for three blood glucose concentrations. The panels on the left, middle and right columns refer to δ_{skin}, δ_{fat} set according to the minimum, average and maximum values reported in TAB. 2, respectively. For each cases, the skin and fat layer dielectric/conductivity properties have been set to the nominal values (i.e., the average values reported in TAB. 1). Finally, the properties of the blood for the three different concentrations has been set as reported in TAB. 3.

To better appreciate the role of the loading layer the comparison must be cast in quantitative terms. This is achieved here by resorting to the performance metrics introduced previously by considering all the described sensors.

The behaviour of the sensor resolution *SR* is reported in TABS. 4 and 5 which corresponds to the different perturbed phantoms basically by following the same rationale as employed in Figs. 5 and 6, respectively. Inspecting such tables it can be noted that different sensors show different resolution. This of course is to be expected, and indeed, most of the research on microwave sensors just addresses new sensor's topology for improving this resolution. However, here, the focus is on the role played by the loading layer in mitigating the effect of tissues' uncertainties. In this regard, what can be grab by such tables, is that the loading layer tends to reduce the resolution. This matches intuition for since if the superstrate is to make the sensor resilient to change in the tissues unavoidably it will reduce

TABLE 4. Sensor resolution *SR* [MHz/mg/dl] for fixed layer thicknesses set at the nominal values (i.e., average values in TAB.2).

	Patch Antenna		Patch Resonator		Split Ring Resonator	
Tissue Properties	PA	LPA	PR	LPR	SRR	LSRR
$\epsilon, \sigma_{skin-fat_{min}}$	0.1400	0.0112	0.0300	0.0050	0.0085	0.0090
$\epsilon, \sigma_{skin-fat_{av}}$	0.1500	0.0880	0.0400	0.0037	0.0070	0.0095
$\epsilon, \sigma_{skin-fat_{max}}$	0.1500	0.0075	0.0400	0.0075	0.0545	0.0065

TABLE 5. Sensor resolution *SR* [MHz/mg/dl] for tissues' properties set at the nominal values (i.e., average values in TAB.1).

	Patch Antenna		Patch Resonator		Split Ring Resonator	
Tissue Thicknesses	PA	LPA	PR	LPR	SRR	LSRR
$\delta_{skin-fat_{min}}$	0.1600	0.0050	0.0400	0.0050	0.0085	0.0090
$\delta_{skin-fat_{av}}$	0.0800	0.0138	0.0100	0.0063	0.0055	0.0100
$\delta_{skin-fat_{max}}$	0.0400	0.0075	0.0200	0.0063	0.0140	0.0200

TABLE 6. Q factor for fixed layer thicknesses set at the nominal values (i.e., average values in TAB.2).

	$BGC = 100$ [mg/dl]						$BGC = 200$ [mg/dl]					
Tissue Properties	PA	PLA	PR	LPR	SRR	LSRR	PA	PLA	PR	LPR	SRR	LSRR
$\epsilon, \sigma_{skin-fat_{min}}$	2.40	11.61	15.21	41.82	159.80	171.88	2.54	117.21	15.43	42.28	159.00	170.44
$\epsilon, \sigma_{skin-fat_{av}}$	2.38	113.03	15.06	41.45	160.22	171.89	2.51	118.78	15.49	41.82	159.38	170.93
$\epsilon, \sigma_{skin-fat_{max}}$	2.41	108.86	14.66	41.10	159.11	169.96	2.52	114.20	15.27	41.65	158.94	170.00
	$BGC = 300$ [mg/dl]											
Tissue Properties	PA	PLA	PR	LPR	SRR	LSRR						
$\epsilon, \sigma_{skin-fat_{min}}$	2.67	136.10	16.49	42.27	158.57	170.47						
$\epsilon, \sigma_{skin-fat_{av}}$	2.65	140.32	16.82	41.65	158.98	170.47						
$\epsilon, \sigma_{skin-fat_{max}}$	2.65	132.10	16.58	42.20	158.55	160.51						

TABLE 7. Q factor for tissue properties set at the nominal values (i.e., average values in TAB.1).

	$BGC = 100$ [mg/dl]						$BGC = 200$ [mg/dl]					
Tissue Properties	PA	PLA	PR	LPR	SRR	LSRR	PA	PLA	PR	LPR	SRR	LSRR
$\delta_{skin-fat_{min}}$	2.44	110.22	17.52	41.27	158.11	171.37	2.58	118.68	18.07	42.00	158.14	170.43
$\delta_{skin-fat_{min}}$	2.44	264.74	10.52	44.10	158.12	170.81	2.58	250.30	10.34	44.51	158.13	169.94
$\delta_{skin-fat_{min}}$	2.44	660.86	8.21	44.50	156.41	171.32	2.58	562.55	8.17	45.26	156.40	169.48
	$BGC = 300$ [mg/dl]											
Tissue Properties	PA	PLA	PR	LPR	SRR	LSRR						
$\delta_{skin-fat_{min}}$	2.70	142.40	19.56	42.19	157.32	169.48						
$\delta_{skin-fat_{min}}$	2.70	289.22	10.08	44.94	157.32	169.00						
$\delta_{skin-fat_{min}}$	2.68	420.27	7.73	45.38	157.31	169.03						

sensitivity to change occurring in the blood layer as well. This seems to not hold true for the SRR, maybe because in this case the superstrate is much smaller than for the other two sensors. However, the loss in resolution can be can be remedied by employing specific signal processing techniques [32], [33], we once again points out that here we are mainly interested in sensors exhibiting a relatively stable response while the tissues properties change.

The corresponding Q factors are reported in TABS. 6 and 7. In this case, the superstrate has a positive effect and allows to significantly increase the Q factor. Once again, the SRR seems to be less sensitive to the introduction of the superstrate.

Finally, we turn to address the stability of the sensors' responses. To this end, the RM metric is reported in TABS. 8 and 9. It can be seen that the loading superstrate actually allows to obtain much more stable resonance frequencies. In particular, for a given blood glucose concentration the maximum deviation of the resonance frequency normalized to the nominal one is of one and two orders of magnitude lower for the case of LPA and LPR, respectively. However, for the SRR sensor RM is almost the same. This is

TABLE 8. Sensor robustness *RM* against skin and fat dielectric/conductivity perturbations as in TAB. 4 while the tissues' thicknesses are set at their nominal values.

	Patch Antenna		Patch Resonator		Split Ring Resonator	
BGC [mg/dl]	PA	LPA	PR	LPR	SRR	LSRR
100	1.217	0.163	3.667	0.031	0.168	0.018
200	1.217	0.163	3.667	0.031	0.025	0.018
300	1.217	0.152	3.583	0.031	0.015	0.010

TABLE 9. Sensor robustness *RM* against skin and fat thickness variations as in TAB. 5 for dielectric and conductivity properties set at the nominal values.

	Patch Antenna		Patch Resonator		Split Ring Resonator	
BGC [mg/dL]	PA	LPA	PR	LPR	SRR	LSRR
100	0.696	0.152	3.583	0.052	0.033	0.030
200	0.348	0.109	3.583	0.042	0.027	0.013
300	0.521	0.098	3.833	0.063	0.010	0.013

probably due to the small sensing area and then to smaller sample phantom used which is deemed to affect at much lower extent the sensor's response.

Eventually, the presented analysis confirms that using a supestrate loading layer allows to strongly mitigate the fluctuation of the resonance frequency against phantom tissue uncertainties. Also, the Q factor is generally increased. However, this happens at the cost of a reduced resolution.

V. CONCLUSION AND FUTURE DEVELOPMENTS

In the framework of microwave sensors design for blood glucose monitoring, the effect of tissues properties uncertainties on the sensor response has been analyzed and faced in this work. In particular, it has been shown that the above uncertainties lead the resonance frequency to deviate from the expected one. In addition, the deviation is not systematic, and hence it cannot be compensated by a calibration procedure. This situation can clearly lead to wrong glucose level estimations.

In order to mitigate such a drawback, the possibility to introduce a loaded superstrate layer has been considered. To introduce a generally applicable methodology, three different microwave sensors configurations taken from literature have been considered and specifically optimized to achieve a stable response.

In order to quantitatively assess the role of the loaded layer, three metrics have been considered, namely: the resolution and the Q factor, commonly adopted in literature, and a robustness measure of the sensor. This latter, in particular, measures the deviation of the resonance frequency, for a fixed blood glucose concentration, while the tissues properties are perturbed as compared to the nominal ones.

Numerical results have shown that the proposed superstrate can significantly improve the sensor robustness, even by two orders of magnitude. Nonetheless, the actual gain depends on the sensor type and the related sensing area size. As an example, for a SRR sensor, the role of the superstrate is revealed to be marginal. The loaded layer has been also demonstrated to allow an increase in the Q factor, but at the expense of a reduced resolution.

The study reported in this manuscript should be considered as a first proof of concept, and further analysis may be performed for future developments. For example, a simple numerical optimization procedure has been applied in this work, by uniquely exploiting the superstrate thickness as a degree of freedom. If considering in the future also the optimization of the superstrate dielectric permittivity, improved results are expected. In addition, a planar numerical phantom has been considered. A progress should be performed also regarding this point, by considering more realistic phantoms. Another important aspect to be addressed is related to the introduction of an equivalent sensor circuit to model the tissues perturbations and the superstrate effect. However, while the circuit topology is relatively easy to establish, the dependence of the circuit element on the medium electromagnetic properties is not trivial in the case of a layered medium covering the sensor. Finally, the definitive effectiveness of the proposed strategy must be checked by experimental results.

REFERENCES

[1] *Diabetes Fact Sheet*, World Health Organisation, Geneva, Switzerland, Nov. 2021.

[2] *IDF Diabetes Atlas*, 9th ed., International Diabetes Federation, Brussels, Belgium, 2019.

[3] H. Yao, A. J. Shum, M. Cowan, I. Lähdesmäki, and B. A. Parviz, "A contact lens with embedded sensor for monitoring tear glucose level," *Biosens. Bioelectron.*, vol. 26, no. 7, pp. 3290–3296, Mar. 2011.

[4] J. P. Comer, "Semiquantitative specific test paper for glucose in urine," *Anal. Chem.*, vol. 28, no. 11, pp. 1748–1750, Nov. 1956.

[5] B. Peng, J. Lu, A. S. Balijepalli, T. C. Major, B. E. Cohan, and M. E. Meyerhoff, "Evaluation of enzyme-based tear glucose electrochemical sensors over a wide range of blood glucose concentrations," *Biosens. Bioelectron.*, vol. 49, pp. 204–209, Nov. 2013.

[6] A. Losoya, "State of the art and new perspectives in non-invasive glucose sensors," *Revista Mexicana de Ingenieria Biomedica*, vol. 33, no. 1, pp. 41–52, 2012.

[7] R. A. DeFronzo, R. C. Bonadonna, and E. Ferrannini, "Pathogenesis of NIDDM: A balanced overview," *Diabetes Care*, vol. 15, no. 3, pp. 318–368, Mar. 1992.

[8] T. Karacolak, E. C. Moreland, and E. Topsakal, "Cole-cole model for glucose-dependent dielectric properties of blood plasma for continuous glucose monitoring," *Microw. Opt. Technol. Lett.*, vol. 55, no. 5, pp. 1160–1164, May 2013.

[9] J. Venkataraman and B. Freer, "Feasibility of non-invasive blood glucose monitoring: In-vitro measurements and phantom models," in *Proc. IEEE Int. Symp. Antennas Propag. (APSURSI)*, Jul. 2011, pp. 603–606.

[10] T. Yilmaz, R. Foster, and Y. Hao, "Broadband tissue mimicking phantoms and a patch resonator for evaluating noninvasive monitoring of blood glucose levels," *IEEE Trans. Antennas Propag.*, vol. 62, no. 6, pp. 3064–3075, Jun. 2014.

[11] S. Mustafa, A. M. Abbosh, and P. T. Nguyen, "Modeling human head tissues using fourth-order Debye model in convolution-based three-dimensional finite-difference time-domain," *IEEE Trans. Antennas Propag.*, vol. 62, no. 3, pp. 1354–1361, Mar. 2014.

[12] S. Gabriel, R. W. Lau, and C. Gabriel, "The dielectric properties of biological tissues: III. Parametric models for the dielectric spectrum of tissues," *Phys. Med. Biol.*, vol. 41, no. 11, pp. 2271–2293, Nov. 1996.

[13] S. Costanzo, V. Cioffi, and A. Raffo, "Complex permittivity effect on the performances of non-invasive microwave blood glucose sensing: Enhanced model and preliminary results," in *Trends and Advances in Information Systems and Technologies*, vol. 746. Cham, Switzerland: Springer, 2018, pp. 1505–1511, doi: 10.1007/978-3-319-77712-2_146.

[14] A. Kandwal, L. W. Liu, T. Igbe, J. Li, Y. Liu, R. Das, B. K. Kanaujia, L. Wang, and Z. Nie, "A novel method of using bifilar spiral resonator for designing thin robust flexible glucose sensors," *IEEE Trans. Instrum. Meas.*, vol. 70, pp. 1–10, 2021.

[15] M. Navaei, P. Rezaei, and S. Kiani, "Measurement of low-loss aqueous solutions permittivity with high detection accuracy by a contact and free-label resonance microwave sensor," *Int. J. Commun. Syst.*, vol. 36, no. 5, Mar. 2023, Art. no. e5417.

[16] A. Kandwal, J. Li, T. Igbe, Y. Liu, R. Das, B. K. Kanaujia, and Z. Nie, "Young's double slit method-based higher order mode surface plasmon microwave antenna sensor: Modeling, measurements, and application," *IEEE Trans. Instrum. Meas.*, vol. 71, pp. 1–11, 2022.

[17] P. Vélez, "Single-frequency amplitude-modulation sensor for dielectric characterization of solids and microfluidics," *IEEE Sensors J.*, vol. 21, no. 10, pp. 12189–12201, May 2021.

[18] S. Kiani, P. Rezaei, M. Navaei, and M. S. Abrishamian, "Microwave sensor for detection of solid material permittivity in single/multilayer samples with high quality factor," *IEEE Sensors J.*, vol. 18, no. 24, pp. 9971–9977, Dec. 2018.

[19] A. Ebrahimi, "Highly sensitive phase-variation dielectric constant sensor based on a capacitively-loaded slow-wave transmission line," *IEEE Trans. Circuits Syst. I, Reg. Papers*, vol. 68, no. 7, pp. 2787–2799, Jul. 2021.

[20] P. Velez, "A microwave microfluidic reflective-mode phase-variation sensor," in *Proc. IEEE Sensors*, Oct. 2021, pp. 1–4.

[21] S. Kiani, P. Rezaei, and M. Navaei, "Dual-sensing and dual-frequency microwave SRR sensor for liquid samples permittivity detection," *Measurement*, vol. 160, Aug. 2020, Art. no. 107805.

[22] S. Kiani, P. Rezaei, and M. Fakhr, "Dual-frequency microwave resonant sensor to detect noninvasive glucose-level changes through the fingertip," *IEEE Trans. Instrum. Meas.*, vol. 70, pp. 1–8, 2021.

[23] A. A. Oloyo and Z. Hu, "A highly sensitive microwave resonator for non-invasive blood glucose level detection," in *Proc. 12th Eur. Conf. Antennas Propag. (EuCAP)*, Apr. 2018, pp. 1–5.

[24] K. K. Adhikari and N. Kim, "Ultrahigh-sensitivity mediator-free biosensor based on a microfabricated microwave resonator for the detection of micromolar glucose concentrations," *IEEE Trans. Microw. Theory Techn.*, vol. 64, no. 1, pp. 319–327, Jan. 2016.

[25] K. K. Adhikari, Z. Chuluunbaatar, H. Park, Y. Jung, G. Cho, Y. H. Jo, S. S. Kim, and N. Y. Kim, "Flexible screen printed biosensor with high-Q microwave resonator for rapid and sensitive detection of glucose," in *IEEE MTT-S Int. Microw. Symp. Dig.*, Dec. 2014, pp. 1–3.

[26] C. Jang, J.-K. Park, H.-J. Lee, G.-H. Yun, and J.-G. Yook, "Temperature-corrected fluidic glucose sensor based on microwave resonator," *Sensors*, vol. 18, no. 11, p. 3850, Nov. 2018.

[27] B. Camli, E. Kusakci, B. Lafci, S. Salman, H. Torun, and A. D. Yalcinkaya, "Cost-effective, microstrip antenna driven ring resonator microwave biosensor for biospecific detection of glucose," *IEEE J. Sel. Topics Quantum Electron.*, vol. 23, no. 2, pp. 404–409, Mar. 2017.

[28] S. Costanzo, "Non-invasive microwave sensors for biomedical applications: New design perspectives," *Radioengineering*, vol. 26, no. 2, pp. 406–410, Jun. 2017.

[29] S. Costanzo, "Loss tangent effect on the accurate design of microwave sensors for blood glucose monitoring," in *Proc. 11th Eur. Conf. Antennas Propag. (EUCAP)*, Mar. 2017, pp. 661–663.

[30] M. Abdolrazzaghi, N. Katchinskiy, A. Y. Elezzabi, P. E. Light, and M. Daneshmand, "Noninvasive glucose sensing in aqueous solutions using an active split-ring resonator," *IEEE Sensors J.*, vol. 21, no. 17, pp. 18742–18755, Sep. 2021.

[31] M. Abdolrazzaghi, R. Genov, and G. V. Eleftheriades, "Microwave planar sensor antenna for glucose sensing in aqueous solutions," in *Proc. IEEE Int. Symp. Antennas Propag. USNC-URSI Radio Sci. Meeting (APS/URSI)*, Dec. 2021, pp. 127–128.

[32] G. Buonanno, A. Brancaccio, S. Costanzo, and R. Solimene, "Response sharpening of resonant sensors for potential applications in blood glucose monitoring," *IEEE J. Electromagn., RF Microw. Med. Biol.*, vol. 6, no. 2, pp. 287–293, Jun. 2022, doi: 10.1109/JERM.2022.3152061.

[33] G. Buonanno, A. Brancaccio, S. Costanzo, and R. Solimene, "Spectral methods for response enhancement of microwave resonant sensors in continuous non-invasive blood glucose monitoring," *Bioengineering*, vol. 9, no. 4, p. 156, Apr. 2022, doi: 10.3390/bioengineering9040156.

[34] S. Costanzo, G. Buonanno, and R. Solimene, "Super-resolution spectral approach for the accuracy enhancement of biomedical resonant microwave sensors," *IEEE J. Electromagn., RF Microw. Med. Biol.*, vol. 6, no. 4, pp. 539–545, Dec. 2022, doi: 10.1109/JERM.2022.3210457.

[35] G. Buonanno, S. Costanzo, A. Cuccaro, and R. Solimene, "Method for robust estimation of the resonance frequency of microwave biosensors," in *Proc. 17th Eur. Conf. Antennas Propag. (EuCAP)*, Mar. 2023, pp. 1–3.

[36] H. Choi, J. Nylon, S. Luzio, J. Beutler, and A. Porch, "Design of continuous non-invasive blood glucose monitoring sensor based on a microwave split ring resonator," in *IEEE MTT-S Int. Microw. Symp. Dig.*, Dec. 2014, pp. 1–3.

[37] V. Turgul and I. Kale, "Influence of fingerprints and finger positioning on accuracy of RF blood glucose measurement from fingertips," *Electron. Lett.*, vol. 53, no. 4, pp. 218–220, Feb. 2017.

[38] S. Kiani, P. Rezaei, M. Karami, and R. Sadeghzadeh, "Band-stop filter sensor based on SIW cavity for the non-invasive measuring of blood glucose," *IET Wireless Sensor Syst.*, vol. 9, no. 1, p. 15, 2019.

[39] A. Cuccaro, A. Dell'Aversano, G. Buonanno, S. Costanzo, and R. Solimene, "Design strategy of microwave resonant sensors with stable response for blood glucose monitoring," in *Proc. 17th Eur. Conf. Antennas Propag. (EuCAP)*, Mar. 2023, pp. 1–5.

[40] K. Sen and S. Anand, "Design of microstrip sensor for non invasive blood glucose monitoring," in *Proc. Int. Conf. Emerg. Trends Innov. ICT (ICEI)*, Feb. 2017, pp. 5–8.

[41] T. Yilmaz, A. Brizzi, R. Foster, M. Munoz, and Y. Hao, "A patch resonator for sensing blood glucose changes," in *Proc. 31st URSI Gen. Assem. Sci. Symp. (URSI GASS)*, Aug. 2014, pp. 1–4.

[42] M. Navaei, P. Rezaei, and S. Kiani, "Microwave split ring resonator sensor for determination of the fluids permittivity with measurement of human milk samples," *Radio Sci.*, vol. 57, no. 7, pp. 1–11, Jul. 2022.

[43] S. Costanzo and V. Cioffi, "Dielectric models for the accurate design of wearable diabetes sensors," in *Proc. 23rd Int. Conf. Appl. Electromagn. Commun. (ICECOM)*, Sep. 2019, pp. 1–3.

[44] T. Lin, "Non-invasive glucose monitoring: A review of challenges and recent advances," *Current Trends Biomed. Eng. Biosci.*, vol. 6, no. 5, pp. 1–8, Jul. 2017.

[45] K. S. Cole and R. H. Cole, "Dispersion and absorption in dielectrics I. Alternating current characteristics," *J. Chem. Phys.*, vol. 9, no. 4, pp. 341–351, Apr. 1941.

[46] T. Yilmaz, R. Foster, and Y. Hao, "Radio-frequency and microwave techniques for non-invasive measurement of blood glucose levels," *Diagnostics*, vol. 9, no. 1, p. 6, Jan. 2019.

[47] M. F. A. M. Yunos, R. Manczak, C. Guines, A. F. M. Mansor, W. C. Mak, S. Khan, N. A. Ramli, A. Pothier, and A. N. Nordin, "RF remote blood glucose sensor and a microfluidic vascular phantom for sensor validation," *Biosensors*, vol. 11, no. 12, p. 494, Dec. 2021, doi: 10.3390/bios11120494.

[48] N. Kazemi and P. Musilek, "Enhancing microwave sensor performance with ultrahigh Q features using CycleGAN," *IEEE Trans. Microw. Theory Techn.*, vol. 70, no. 12, pp. 5369–5382, Dec. 2022.

[49] [Online]. Available: https://www.avient.com/products/engineered-polymer-formulations/conductive-signal-radiation-shielding-formulations/preperm-low-loss-dielectric-thermoplastics

SANDRA COSTANZO (Senior Member, IEEE) received the Laurea degree (summa cum laude) in computer engineering from Universitã della Calabria, Italy, in 1996, and the Ph.D. degree in electronic engineering from Universitã Mediterranea di Reggio Calabria, Italy, in 2000. Since 2019, she has been an Associate Professor with IREA-CNR (Naples). She is currently an Associate Professor with Universitã della Calabria, where she is also the Coordinator of master's degree in telecommunication engineering and the Rector's Delegate for security, protection, and control of electromagnetic fields. She teaches courses on electromagnetic wave propagation, antennas, remote sensing, radar, sensors, and electromagnetic diagnostics. She has authored or coauthored more than 200 contributions in international journals, books, and conferences. Her current research interests include near-field/far-field techniques, antenna measurement techniques, antenna analysis and synthesis, numerical methods in electromagnetics, millimeter wave antennas, reflectarrays, synthesis methods for microwave structures, electromagnetic characterization of materials, biomedical applications, and radar technologies. She is a member of the IEEE MTT-28 Biological Effects and Medical Applications Committee, IEEE South Italy Geoscience and Remote Sensing Chapter, Consorzio Nazionale Interuniversitario per le Telecomunicazioni (CNIT), Societã Italiana di Elettromagnetismo (SIEM), and Centro Interuniversitario sulle Interazioni fra Campi Elettromagnetici e Biosistemi (ICEMB); and a Board Member of the IEEE AP/ED/MTT North Italy Chapter. She received the Telecom Prize for the Best Laurea Thesis, in 1996, and the 2013 Best Academia and Research Application in Aerospace and Defense Award for the application of software-defined radar using the NI USRP 2920 platform. In 2017, she awarded the Italian National Scientific Qualification for the Full Professor position. She is an Associate Editor of IEEE Access, IEEE Journal of Electromagnetics, RF and Microwaves in Medicine and Biology, and *Electronics* (section ''Microwave and Wireless Communications''). She is an Editorial Board Member of *Radioengineering* and *International Journal of RF and Microwave Computer-Aided Engineering*. She is an Editor of the books *Microwave Materials Characterization* (INTECH, 2012) and *Wave Propagation Concepts for Near-Future Telecommunication Systems* (INTECH, 2017). She was a Lead Editor of the Special Issues on *Reflectarray Antennas: Analysis and Synthesis Techniques*, in 2012, *Advances in Radar Technologies*, in 2013, *Compressed Sensing: Applications in Radar and Communications*, in 2016, *Bioengineering Applications of Electromagnetic Wave Propagation*, in 2019, and *Microwave Sensors for Biomedical Applications*, in 2020.

ANTONIO CUCCARO received the Laurea (summa cum laude) and Ph.D. degrees in electronic engineering from Seconda Universitã degli Studi di Napoli (SUN), Aversa, Italy, in 2012 and 2015, respectively. Then, he joined the Research Group in Applied Electromagnetic, SUN. Then, he was a Research Fellow with the University of Campania ''Luigi Vanvitelli.'' He is currently a Researcher with the Department of Informatics, Modeling, Electronics and Systems Engineering (DIMES), Universitã della Calabria. His current research interests include through-the-wall imaging applications, biomedical imaging, and antenna design and diagnostics.

ANGELA DELL'AVERSANO received the Laurea (summa cum laude) and Ph.D. degrees in electronic engineering from Seconda Universitã degli Studi di Napoli (SUN), Aversa, Italy, in 2012 and 2014, respectively. Then, she joined the Research Group in Applied Electromagnetic, SUN. She is currently a Research Fellow with Universitã della Campania ''Luigi Vanvitelli.'' Her current research interests include inverse scattering problems and microwave imaging.

GIOVANNI BUONANNO (Member, IEEE) received the M.S. degree (summa cum laude) in electronic engineering from Seconda Universitã degli Studi di Napoli (SUN), Aversa, Italy, in 2014, and the Ph.D. degree in industrial and information engineering with the University of Campania, in 2018. Then, he joined the Research Group in Applied Electromagnetics, SUN. He defending the Ph.D. thesis, in January 2019. He is currently a Researcher with the University of Calabria. His current research interests include nonuniformly-spaced random arrays, biomedical signal processing, machine learning in electromagnetics, and the tolerance analysis of antenna arrays.

RAFFAELE SOLIMENE (Senior Member, IEEE) received the Laurea (summa cum laude) and Ph.D. degrees in electronic engineering from Seconda Università degli Studi di Napoli (SUN), Aversa, Italy, in 1999 and 2003, respectively. In 2002, he was an Assistant Professor with the Faculty of Engineering, Mediterranea University of Reggio Calabria, Italy. Since 2006, he has been with Dipartimento di Ingegneria, University of Campania ''Luigi Vanvitelli,'' where he is currently a Full Professor. He has an adjunct position with the Indian Institute of Technology Madaras, Chennai, India. His current research interests include inverse electromagnetic problems with applications to inverse source and inverse scattering, non-destructive subsurface investigations, through-the-wall and GPR imaging, microwave medical imaging, array diagnostics, and random arrays. On these topics, he has authored/coauthored more than 250 scientific works, routinely serves as a reviewer for several journals, and organized several scientific sessions. He is a member of Societã Italiana di Elettromagnetismo (SIEM), Consorzio Nazionale Interuniversitario per le Telecomunicazioni (CNIT), and Centro Interuniversitario sulle Interazioni fra Campi Elettromagnetici e Biosistemi (ICEMB). He is an Associate Editor of IEEE Geoscience and Remote Sensing Letters, *Mathematical Problems in Engineering*, and *International Journal of Antennas and Propagation and Electronics* (section ''Microwave and Wireless Communications'').

Open Access funding provided by 'Università della Calabria' within the CRUI CARE Agreement